RSC Advances

PAPER

View Article Online
View Journal | View Issue

Cite this: *RSC Adv.*, 2017, **7**, 39611

An electrochemical sensor based on Co_3O_4 nanosheets for lead ions determination†

Lei Yu,[a] Ping Zhang,[a] Hongxiu Dai,[b] Ling Chen,[c] Houyi Ma,[b] Meng Lin*[b] and Dazhong Shen*[a]

Received 5th June 2017
Accepted 7th August 2017

DOI: 10.1039/c7ra06269a

rsc.li/rsc-advances

In this work, Co_3O_4 nanosheets were fabricated on indium tin oxide (ITO) substrates by developing a simple electrochemical deposition and annealing method. The as-prepared Co_3O_4 nanosheets were characterized by scanning electron microscopy (SEM), X-ray diffraction (XRD), attenuated total reflection infrared (ATR-IR) spectroscopy and Raman spectroscopy. The Co_3O_4 nanosheets modified ITO electrode was used for the electrochemical analysis of various trace lead ions by differential pulse anodic stripping voltammetry. The electrode was found to be highly selective to Pb(II) in the range of 1–100 μg L^{-1}, and exhibited a sensitive current response with a limit of detection (LOD) of 0.52 μg L^{-1}. Furthermore, the developed electrochemical Pb(II) sensor exhibited a high stability and reproducibility with a simple regeneration process.

1 Introduction

Heavy metal ions, such as Pb(II), Cu(II) and Hg(II), have become of increasing worldwide concern as important hazardous pollutants of the environment and human health at low concentration, because of their high toxicity and latent carcinogenicity.[1] Pb(II) in drinking water generates health problems at even low concentrations, such as digestive, neurological, cardiac and mental troubles, especially to the elderly and children.[2] Hence, a number of analytical methods for Pb(II) detection have been reported, such as plasma-optical emission spectrometry,[3] flame atomic absorption spectrometry[4] and X-ray fluorescence spectrometry,[5] though these techniques all involve requirements of sophisticated instruments, high operating costs and complicated procedures. Comparatively, electrochemical methods, particularly anodic stripping voltammetry analysis, have become one of the most commonly used methods for detecting trace heavy metal ions due to their high sensitivity, low cost, ease of sample preparation, fast analysis speed and portability.[1]

Most of the literature about the electrochemical detection of metal ions is usually focused on using noble metals, carbon or silicon-based composites or organic molecules as the electrode's modified materials.[1] For example, Sahoo *et al.* developed an gold nanoparticles modified electrode for simultaneous determination of Cu(II) and Hg(II);[6] Promphet and co-works used graphene/polyaniline/polystyrene nanoporous fiber-modified SPCE for the simultaneous determination of Pb(II) and Cd(II);[7] Huang *et al.* reported the simultaneous determination of Cd(II) and Pb(II) by using graphene oxide-walled carbon nanotubes composites as the sensing material.[8] However, these functionalized materials for detection of heavy metal ions are expensive or required complex synthesis processes.

During recent decades, metal oxides have remarkably facilitated great progresses in a broad range of scientific fundamentals and technological potentials.[9] Cobalt oxide (Co_3O_4) nanostructures are one of the promising metal oxide materials which have found wide applications in electrochemical biosensors,[10,11] electrochromic devices,[12] supercapacitors,[13] batteries.[14] Due to the electrochemical stability and adsorption capacity, Co_3O_4 nanocrystals synthesized *via* a hydrothermal process were used for the detection of Pb(II).[15] However, the synthetic method of Co_3O_4 suffered from the complications of the complex synthesis process and needed organic additives. Therefore, it is necessary to develop a mild and easily controlled method for preparing Co_3O_4 nanostructures for metal ions detection. In addition, bismuth film electrode (BiFE) (including *in situ* and *ex situ*) has many excellent properties such as high sensitivity, low electrochemical detection, wide potential window and insensitivity to dissolved oxygen, *etc.*[16] Bismuth based sensors are usually constructed from base materials with a high surface area and pore size to enhance the enrichment of analytes on the electrode surface, such as carbon nanotubes,[16]

[a]*College of Chemistry, Chemical Engineering and Materials Science, Collaborative Innovation Center of Functionalized Probes for Chemical Imaging in Universities of Shandong, The Key Lab in Molecular and Nano-materials Probes of the Ministry of Education of China, Shandong Normal University, Jinan 250014, China. E-mail: dzshen@sdnu.edu.cn; Fax: +86-531-82615258; Tel: +86-531-86180740*

[b]*Key Laboratory for Colloid and Interface Chemistry of State Education Ministry, School of Chemistry and Chemical Engineering, Shandong University, Jinan 250100, China. E-mail: mlin@sdu.edu.cn; Fax: +86-531-88564464; Tel: +86-531-88369996*

[c]*School of Materials Science and Engineering, University of Jinan, Jinan 250022, China*

† Electronic supplementary information (ESI) available. See DOI: 10.1039/c7ra06269a

polymers,[17] graphene[18] and Nafion.[19] Till now there are few reports of electrochemical sensor based on the metal oxides and Bi. An iron oxide (Fe_2O_3)/graphene (G) electrode used in combination with *in situ* plated Bi working as an electrochemical sensor for detecting Zn(II), Cd(II), and Pb(II) was reported. The Fe_2O_3/G composite modified electrode offered excellent stability in the electrochemical determination of heavy metal ions due to its high catalytic activity and significantly improved analytical performance.[20]

In the present work, we report a facile electrochemical deposition and annealing process route to obtain the nanostructured Co_3O_4 modified indium tin oxide (ITO) electrode. The developed Co_3O_4 nanosheets modified electrode was used for sensitive and selective detection towards Pb(II). Electrochemical responses of the Co_3O_4/ITO electrode were investigated using differential pulse anodic stripping voltammetry (DPASV), and the modified electrode proved its capability to determine the concentration of Pb(II) in the range of 1–100 μg L^{-1}. The presence of Co_3O_4 on the electrode surface could enhance the electrochemical activity of the electrode, and the results showed a superior sensitive electrochemical performance for the detection of Pb(II) in real tap water samples by the Co_3O_4/ITO electrode.

2 Experimental

2.1 Reagents and apparatus

All chemical reagents were purchased from Sinopharm Chemical Reagent Co., Ltd. (China) and were of analytical grade. The standard solutions of metal ions were purchased from Aladdin (Shanghai, China). Ultrapure water (>18 MΩ, Ulupure, China) was used throughout the experiments, and all solutions were freshly prepared.

Attenuated total reflection infrared (ATR-IR, Bruker, Germany) spectroscopy and Raman spectroscopy (QE65000) were used to confirm the structural modification of the electrode. The morphology of the nanostructures was characterized by scanning electron microscope (SEM, HITACHI-S4700). X-ray powder diffraction (XRD) patterns were recorded using a Bruker D8 advanced X-ray diffractometer with Cu Kα radiation. All electrochemical measurements were performed on a CHI 650E electrochemistry workstation (Chenhua Instruments, China) with a conventional three-electrode system comprising the modified electrode as a working electrode, a saturated calomel electrode (SCE) as a reference electrode and a large platinum plate as a counter electrode.

2.2 Preparation of the Co_3O_4/ITO electrode

Co_3O_4/ITO electrode was prepared by a simple electrodeposition process. Prior to the electrodeposition, the ITO glass (0.8 × 5 cm^2) was sonicated in acetone, ethanol and ultrapure water for 15 min, respectively. $Co(OH)_2$ nanosheets were electrochemical deposited on the surface of ITO glass at −1.0 V (*versus* SCE) in 0.1 M $Co(NO_3)_2$ aqueous solution. In order to obtain the desired crystalline phase of Co_3O_4, the as-prepared $Co(OH)_2$/ITO electrode film was calcined in air at the rate of 2 °C min^{-1} from room temperature to 300 °C and maintained at 300 °C for 2 h.

2.3 Electrochemical measurement

In the detection of Pb(II) by DPASV, 0.1 M NaAc–HAc buffer of pH = 5.0 containing 400 μg L^{-1} bismuth was employed as the supporting electrolyte. Firstly, the Co_3O_4/ITO electrode was immersed into a NaAc–HAc buffer solution containing various concentration of Pb(II) ions, and then reduction of Pb(II) ions into Pb under a constant potential at −1.0 V for 200 s. Subsequently, the electrochemical behavior of the Co_3O_4/ITO electrode was measured by DPASV in the range from −0.75 to −0.45 V with an amplitude of 50 mV, and step increment of 4 mV in a metal ions-free buffer solution. After detection, the modified electrode was regenerated at a desorption potential of 0.4 V for 1 min under stirring to remove the residual metal ions.

3 Results and discussion

3.1 Characterization

Co_3O_4 nanosheets were prepared on the ITO substrate by the electrochemical deposition and annealing process. The electrodeposition process of the $Co(OH)_2$ contained electrochemical and precipitation reaction steps. The Co^{2+} in the solution reacted with OH^- at the anode, meanwhile NO_3^- reacted with H_2O at the cathode, forming $Co(OH)_2$ expressed as follows[21]

$$NO_3^- + H_2O + 2e^- \rightarrow NO_2^- + 2OH^- \quad (1)$$

$$Co^{2+} + 2OH^- \rightarrow Co(OH)_2 \quad (2)$$

Compared with glassy carbon electrode (GCE) and screen printed electrodes (SPEs), indium tin oxide (ITO) is a transparent conductor and cost-effective material, has good stability and durability below 500 °C.[22] Therefore, ITO glass was chosen as the electrode substrate for preparation of the nanostructured Co_3O_4. After heat treatment, the colour of the modified electrode was changed from green to dark black because of the transformation of $Co(OH)_2$ into Co_3O_4.[22] Fig. 1 illustrates the SEM images of the $Co(OH)_2$ and Co_3O_4 nanosheets. It can be seen that the $Co(OH)_2$ nanosheets have a layered and porous structure, which is similar to CdI_2 type layered structure with

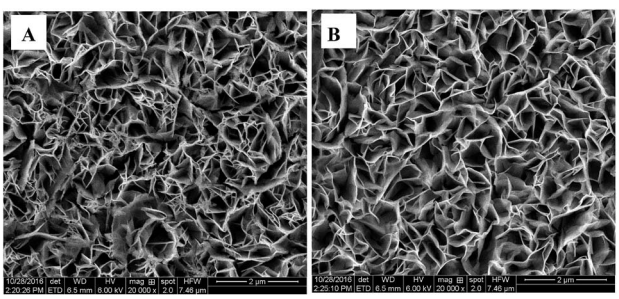

Fig. 1 SEM images of the $Co(OH)_2$ nanosheets (A) and the Co_3O_4 nanosheets (B).

weak interaction between layers and strong binding within the layered planes, indicating that the $Co(OH)_2$ nanosheets were grown preferentially along the layered plane to form two dimensional nanosheet structure.[23] As Fig. 1B shown, the $Co(OH)_2$ nanosheets converted into the Co_3O_4 nanosheets through the annealing process, and the morphology of Co_3O_4 remained almost similar to that of $Co(OH)_2$.

Fig. 2 shows the XRD patterns of the $Co(OH)_2$ and Co_3O_4 nanosheets films. The powder XRD pattern of the $Co(OH)_2$ nanosheets shows three small diffraction peaks at 10.6, 35.2, and 60.8° in the range of 10 to 80°, which could be indexed to (001), (100) and (110) reflections of a hydrotalcite-like low-crystalline α-$Co(OH)_2$ structure.[24] The Co_3O_4 nanosheets show diffraction peaks at 19.0, 31.4, 36.8, 59.2 and 65.3°, which correspond to (111), (220), (311), (511) and (440) crystal planes of spinel Co_3O_4 phase,[25] respectively, indicating that the crystalline Co_3O_4 films were formed after heat treatment. The change of composition and phase is confirmed further by ATR-IR and Raman measurements.

Fig. 3A displays the ATR-IR spectra of $Co(OH)_2$ and Co_3O_4. For $Co(OH)_2$ nanosheets, the peak of the centered at 630 cm^{-1} could be assigned to the Co–OH stretching vibration, and those in the 1400–1500 cm^{-1} range according to the bending vibrations of adsorbed water molecules.[26] For Co_3O_4 nanosheets, two high characteristic peaks at 662 cm^{-1} and 567 cm^{-1} are corresponded to the vibration peaks of Co^{2+}–O and Co^{3+}–O bonds, respectively.[27] After calcination, the 1400 cm^{-1} peaks in $Co(OH)_2$ disappear completely, indicating the conversion of $Co(OH)_2$ to Co_3O_4.[28] As shown in Fig. 3B, five obvious peaks are exhibited at 194, 477, 514, 616, and 684 cm^{-1} in the Raman spectrum of Co_3O_4, which correspond to F^1_{2g}, E_g, F^2_{2g}, F^3_{2g} and A_{1g} Raman active vibration modes.[29] However, the Raman spectral peaks of the $Co(OH)_2$ do not appear owing to the short time of the electrodeposited treatment.

3.2 Electrochemical performance of the modified electrodes

Optimization for electrochemical detection of Pb(II) by the Co_3O_4 nanosheets were investigated in Fig. S1,† and 4 shows the DPASV responses towards Pb(II) at the bare ITO, $Co(OH)_2$/ITO, and Co_3O_4/ITO electrodes. It can be seen that there are slight

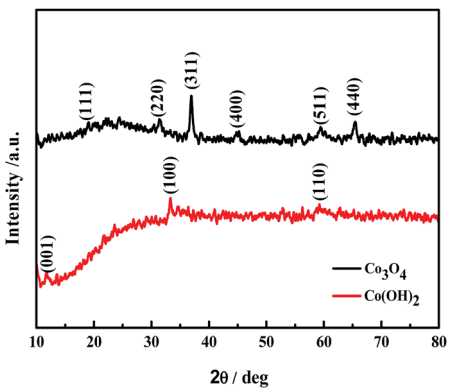

Fig. 2 XRD patterns of $Co(OH)_2$ and Co_3O_4.

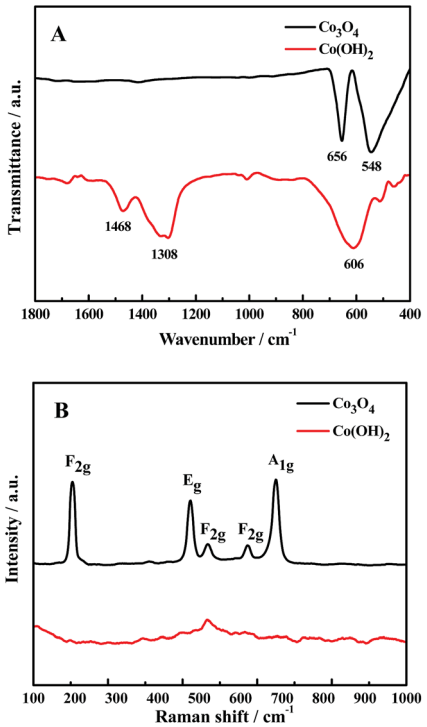

Fig. 3 ATR-IR spectra (A) and Raman spectra (B) of $Co(OH)_2$ and Co_3O_4.

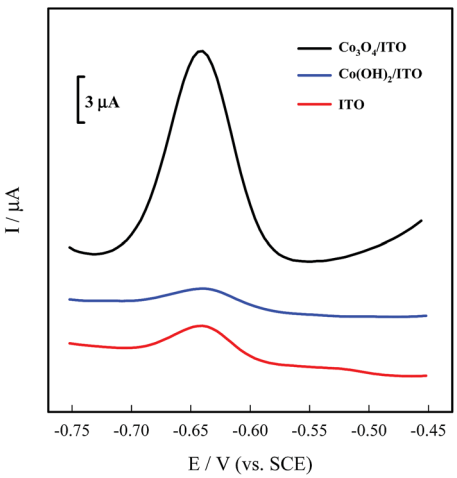

Fig. 4 DPASV of ITO, $Co(OH)_2$/ITO and Co_3O_4/ITO electrodes in 0.1 M NaAc–HAc buffer (pH 5.0) containing 20 μg L^{-1} Pb(II) and 400 μg L^{-1} Bi(III). Deposition potential: −1.0 V, deposition time: 200 s, amplitude: 0.05 V, increment potential: 0.004 V, pulse width: 0.05 s, pulse period: 0.2 s.

peaks for the bare ITO and $Co(OH)_2$/ITO electrodes appeared. On the contrary, a strong and well-defined response at −0.64 V is clearly obtained for the Co_3O_4/ITO electrode, which confirmed that the modification of the Co_3O_4 nanosheets can significantly improve the sensitivity towards Pb(II) ions. Fig. S2† displays the DPASV responses at the Co_3O_4/ITO electrode with and without Bi(III). The electrochemical signal on the modified electrode containing Bi(III) is notably improved by about 2.5

times for detecting Pb(II) than that of the absence of Bi(III) system, which is attributed to the capacity of bismuth to form a "fused alloy" with trace metal ions, resulting in easier reduction of Pb(II).[30]

We investigated the DPASV response of various concentration of Pb(II) ions at the Co_3O_4 nanosheets modified ITO electrode between −0.75 and −0.45 V. Fig. 5 shows the DPASV peaks originating from the Co_3O_4/ITO electrode, and the peak currents increased with the increasing concentration of Pb(II) in the range of 1–100 μg L^{-1}. The linear regression equation is expressed by ΔI_p (μA) = 1.2971 + 0.65227C_{pb} (μg L^{-1}) (R^2 = 0.999). F value is 2.68, which is smaller than the 5% point of $F_{7,9}$ (3.29). Therefore, there is no significant lack-of-fit, and a linear relationship between concentration and signal. Limit of quantity (LOQ) and limit of detection (LOD) are calculated to be 1.58 ± 0.08 μg L^{-1} (S/N = 10) and 0.52 ± 0.02 μg L^{-1} (S/N = 3.29), respectively, which was comparable to the previously literatures in Table 1. The LOD of the prepared sensor was far below the guideline values of 10 μg L^{-1} for Pb(II) in drinking water given by the World Health Organization.[15]

The interference study containing 20 μg L^{-1} Pb(II) with other potential interfering metal ions (including 200 μg L^{-1} K(I), Mg(II), Ca(II), Fe(III), Mn(II), Zn(II) and Cu(II)) was performed and summarized in Table 2 and Fig. S3.† As expected, these ions except Cu(II) had no significant effect on the determination of Pb(II). The stripping current of Pb(II) ions were changed by 25.2% when the addition of 10-fold Cu(II) ions. When the concentration of Cu(II) was similar to that of the target ion Pb(II) (20 μg L^{-1}), the peak current of Pb(II) was changed little. Such interference was similar to that reported literature for other electrode.[37] Hence, it was reasonable to expect the potential application of the Co_3O_4/ITO electrode for Pb(II) detection. Moreover, the reproducibility of the electrochemical sensor was investigated by DPASV, and the result was found to be excellent as evidenced by a relative standard deviation of 5.1% from seven different modified electrodes.

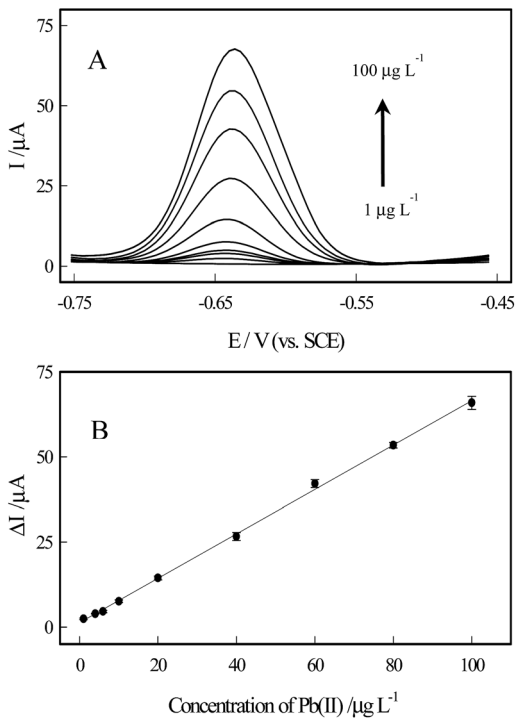

Fig. 5 Typical DPASV responses (A) and the corresponding calibration plots (B) of the Co_3O_4/ITO electrode towards Pb(II) at different concentrations.

Table 1 A comparison of the different methods reported for the detection of Pb(II)[a]

Methods	Electrode	Linear range (μg L^{-1})	LOD (μg L^{-1})	Ref.
SWASV	Fe_3O_4	60–260	23.8	31
SWASV	MnO_2	20–180	15	32
SWASV	$MnFe_2O_4$	40–220	10.8	33
SWASV	Peptide	10–140	—	34
DPASV	Ag-bipy-CP	4.1–20.7	2.3	35
SWASV	MgO	1–6.7	0.43	36
DPASV	Co_3O_4	1–100	0.52	Present work

[a] SWASV, square wave anodic stripping voltammetry; peptide, CTNTLSNNC(–S–S–); Ag-bipy-CP, Ag-4,4′-bipyridine coordination polymer.

Table 2 Interferences of some metal ions (200 μg L^{-1}) on the stripping peak currents of 20 μg L^{-1} Pb(II)

Interferences	Contribution (%)
K(I)	−1.5
Mg(II)	+4.2
Ca(II)	+4.5
Zn(II)	+5.7
Fe(III)	−4.9
Cu(II)	−25.2
Cd(II)	−4.3
Mn(II)	+2.6

3.3 Reproducibility and stability

The reproducibility of the electrochemical sensor was investigated by DPASV, the result was found to be excellent as evidenced by a relative standard deviation of 5.2% from seven different modified electrodes (Fig. S4†). Fig. S5A and B† illustrate the SEM images of the Co_3O_4 nanosheets through electrochemical deposition of 20 μg L^{-1} Pb(II) and electrochemical removing treatments. It can be seen that their structures of Co_3O_4 had no obvious change before and after stripping, demonstrating the electrochemical analytical process of detecting Pb(II) exerted little effect on the Co_3O_4 nanosheets structure. The DPASV curves of the Co_3O_4 nanosheets before and after stripping processes were provided in Fig. S5C,† indicating that the Pb can be removed completely by the stripping method.

After measurements, the Co_3O_4/ITO modified electrode was rinsed and kept in 0.1 M HAc–NaAc solution (pH = 5.0) at 4 °C, and the electrochemical response of the electrode was tested every 3 days (Fig. S6†), lost only 7.6% of the initial response after

Table 3 Determination of Pb(II) in tap water ($n = 3$), RSD: relative standard deviation

Tap water	Spiked ($\mu g\ L^{-1}$)	Found ($\mu g\ L^{-1}$)	RSD (%)	Recovery (%)
1	10	10.2 ± 0.7	8.4	102
2	20	19.3 ± 1.5	5.3	97
3	50	52.4 ± 2.3	9.2	105

several weeks. The result indicates that the Co_3O_4/ITO modified electrode exhibits a good stability for repetitive electrochemical determination.

3.4 Real sample analysis

In order to evaluate the performance of the Co_3O_4/ITO electrode in the real samples, which replaced the ultrapure water with the tap water, and collected in the laboratory at different times. All the samples were filtered through a 0.2 μm membrane prior to the detection, then diluted by 0.1 M NaAc–HAc buffer of pH = 5.0 containing Bi(III). According to Table 3, the recoveries of Pb(II) from the raw and spiked samples ranged from 97% to 105%, and the relative standard deviation (RSD) was in a range of 5.3–9.2%, which shows the good accuracy of the as-proposed method.

4 Conclusions

In summary, a simple and rapid preparation approach for Co_3O_4/ITO electrode has been developed *via* an electrodeposition and annealing process route. The electrochemical performance of the Co_3O_4/ITO modified electrode, demonstrated for metal ions detection by DPASV in comparison with the other types of modified electrode, proved that the developed sensor is highly sensitive and selective to detect Pb(II). The Co_3O_4/ITO electrode was used for the determination of Pb(II) in the range of 1–100 $\mu g\ L^{-1}$, and detection limited of 0.52 $\mu g\ L^{-1}$. The modified electrode also showed high reproducibility, stability and good electrochemical performance for lead ions detection in real water samples.

Conflicts of interest

There are no conflicts to declare.

Acknowledgements

The authors gratefully acknowledge financial support of the National Natural Science Foundation of China (21275091, 21175084 and 21575080) and Shandong Provincial Natural Science Foundation, China (ZR2017QB004).

Notes and references

1 A. Abbaspour, E. Mirahmadi, A. Khalafi-nejad and S. Babamohammadi, A highly selective and sensitive disposable carbon composite PVC-based membrane for determination of lead ion in environmental samples, *J. Hazard. Mater.*, 2010, **174**, 656–661.
2 H. Sereshti, Y. E. Heravi and S. Samadi, Optimized ultrasound-assisted emulsification microextraction for simultaneous trace multielement determination of heavy metals in real water samples by ICP-OES, *Talanta*, 2012, **97**, 235–241.
3 M. R. Sohrabi, Z. Matbouie, A. A. Asgharinezhad and A. Dehghani, Solid phase extraction of Cd(II) and Pb(II) using a magnetic metal–organic framework, and their determination by FAAS, *Microchim. Acta*, 2013, **80**, 589–597.
4 S. Arzhantsev, X. Li and J. F. Kauffman, Rapid limit tests for metal impurities in pharmaceutical materials by X-ray fluorescence spectroscopy using wavelet transform filtering, *Anal. Chem.*, 2011, **83**, 1061–1068.
5 L. Cui, J. Wu and H. X. Ju, Electrochemical sensing of heavy metal ions with inorganic, organic and bio-materials, *Biosens. Bioelectron.*, 2015, **63**, 276–286.
6 S. Sahoo, A. K. Satpati and A. V. R. Reddy, Electrodeposited Bi–Au nanocomposite modified carbon paste electrode for the simultaneous determination of copper and mercury, *RSC Adv.*, 2015, **5**, 25794–25800.
7 N. Promphet, P. Rattanarat, R. Rangkupan, O. Chailapakul and N. Rodthongkum, An electrochemical sensor based on graphene/polyaniline/polystyrene nanoporous fibers modified electrode for simultaneous determination of lead and cadmium, *Sens. Actuators, B*, 2015, **207**, 526–534.
8 H. Huang, T. Chen, X. Y. Liu and H. Y. Ma, Ultrasensitive and simultaneous detection of heavy metal ions based on three-dimensional graphene–carbon nanotubes hybrid electrode materials, *Anal. Chim. Acta*, 2014, **852**, 45–54.
9 Y. Y. Liang, M. G. Schwab, L. J. Zhi, E. Mugnaioli, U. Kolb, X. L. Feng and K. Mullen, Direct access to metal or metal oxide nanocrystals integrated with one-dimensional nanoporous carbons for electrochemical energy storage, *J. Am. Chem. Soc.*, 2010, **132**, 15030–15037.
10 J. X. Xie, H. Y. Gao, H. Jiang, Y. J. Chen, W. B. Shi, H. Z. Zheng and Y. M. Huang, Co_3O_4–reduced graphene oxide nanocomposite as an effective peroxidase mimetic and its application in visual biosensing of glucose, *Anal. Chim. Acta*, 2013, **796**, 92–100.
11 M. Li, C. Han, Y. F. Zhang, X. J. Bo and L. P. Guo, Facile synthesis of ultrafine Co_3O_4 nanocrystals embedded carbon matrices with specific skeletal structures as efficient non-enzymatic glucose sensors, *Anal. Chim. Acta*, 2015, **861**, 25–35.
12 H. Dai, M. Lin, N. Wang, F. Xu, D. Wang and H. Ma, Nickel-Foam-supported Co_3O_4 nanosheets/PPy nanowire heterostructure for non-enzymatic glucose sensing, *ChemElectroChem*, 2017, **4**, 1135–1170.
13 J. Y. Wang, W. Dou, X. T. Zhang, W. H. Han, X. M. Mu, Y. Zhang, X. H. Zhao, Y. X. Chen, Z. W. Yang, Q. Su, E. Q. Xie, W. Lan and X. R. Wang, Embedded Ag quantum dots into interconnected Co_3O_4 nanosheets grown on 3D graphene networks for high stable and flexible supercapacitors, *Electrochim. Acta*, 2017, **224**, 260–268.
14 W. Zhao, X. Zhou, I. J. Kim and S. Kim, Self-assembled Co_3O_4 hexagonal plates by solvent engineering and their

dramatically enhanced electrochemical performance, *Nanoscale*, 2017, **9**, 940–946.

15 X. Y. Yu, Q. Q. Meng, T. Luo, Y. Jia, B. Sun, Q. X. Li, J. H. Liu and X. J. Huang, Facet-dependent electrochemical properties of Co_3O_4 nanocrystals toward heavy metal ions, *Sci. Rep.*, 2013, **3**, 1–7.

16 X. Xu, L. P. Zeng, S. Xing, Y. Z. Xian, G. Y. Shi and L. T. Jin, Ultrasensitive voltammetric detection of trace lead(II) and cadmium(II) using MWCNTs-nafion/bismuth composite electrodes, *Electroanalysis*, 2008, **24**, 2655–2662.

17 H. X. Dai, N. Wang, D. L. Wang, H. Y. Ma and M. Lin, An electrochemical sensor based on phytic acid functionalized polypyrrole graphene oxide nanocomposites for simultaneous determination of Cd(II) and Pb(II), *Chem. Eng. J.*, 2016, **299**, 150–155.

18 S. Lee, S. Y. Bong, J. H. Ha, M. J. Kwak, S. K. Park and Y. Z. Piao, Electrochemical deposition of bismuth on activated graphene-nafion composite for anodic stripping voltammetric determination of trace heavy metals, *Sens. Actuators, B*, 2015, **215**, 62–69.

19 F. Arduini, J. Q. Calvo, G. Palleschi, D. Moscone and A. Amine, Site synthesis of bismuth nanoparticles for electrochemical determination of lead, *Micro Nano Lett.*, 2010, **7**, 1260–1263.

20 S. Lee, J. Oh, D. Kim and Y. Piao, A sensitive electrochemical sensor using an iron oxide/graphene composite for the simultaneous detection of heavy metal ions, *Talanta*, 2016, **160**, 528–536.

21 X. H. Xia, J. P. Tu, J. Y. Xiang, X. H. Huang, X. L. Wang and X. B. Zhao, Hierarchical porous cobalt oxide array films prepared by electrodeposition through polystyrene sphere template and their applications for lithium ion batteries, *J. Power Sources*, 2010, **195**, 2014–2022.

22 Y. Zhang, Z. Y. Wang, S. Liu and T. Zhang, *In situ* growth of Ag–reduced graphene oxide–carbon nanotube on indium tin oxide and its application for electrochemical sensing, *Mater. Res. Bull.*, 2016, **84**, 355–362.

23 G. X. Pan, X. Xia, F. Cao, P. S. Tang and H. F. Chen, Porous $Co(OH)_2$/Ni composite nanoflake array for high performance supercapacitors, *Electrochim. Acta*, 2012, **63**, 335–340.

24 F. Zhou, Q. L. Liu, J. J. Gu, W. Zheng and D. Zhang, Microwave-assisted anchoring of flowerlike $Co(OH)_2$ nanosheets on activated carbon to prepare hybrid electrodes for high-rate electrochemical capacitors, *Electrochim. Acta*, 2015, **170**, 328–336.

25 C. Y. Yoo, J. Park, D. S. Yun, J. H. Yu, H. Yoon, J. N. Kim, H. C. Yoon, M. Kwak and Y. C. Kang, Crucial role of a nickel substrate in Co_3O_4 pseudocapacitor directly grown on nickel and its electrochemical properties, *J. Alloys Compd.*, 2016, **676**, 407–413.

26 L. A. Saghatforoush, S. Sanati and M. Hasanzadeh, Synthesis, characterization and electrochemical properties of Co_3O_4 nanostructures by using cobalt hydroxide as a precursor, *Res. Chem. Intermed.*, 2015, **41**, 4361–4372.

27 T. Zhou, P. Lu, Z. Zhang, Q. Wang and A. Umar, Perforated Co_3O_4 nanoneedles assembled in chrysanthemum-like Co_3O_4 structures for ultra-high sensitive hydrazine chemical sensor, *Sens. Actuators, B*, 2016, **235**, 457–465.

28 Y. G. Li, B. Tan and Y. Y. Wu, Freestanding mesoporous quasi-single-crystalline Co_3O_4 nanowire arrays, *J. Am. Chem. Soc.*, 2006, **128**, 14258–14259.

29 L. J. Zhang, H. J. Li, K. Z. Li, L. Li, L. F. Wei, L. Feng and Q. G. Fu, Morphology-controlled fabrication of Co_3O_4 nanostructures and their comparative catalytic activity for oxygen evolution reaction, *J. Alloys Compd.*, 2016, **680**, 146–154.

30 F. Arduini, J. Q. Calvo, G. Palleschi, D. Moscone and A. Amine, Bismuth-modified electrodes for lead detection, *Trends Anal. Chem.*, 2010, **29**, 1295–1304.

31 H. L. Fan, S. F. Zhou, J. Gao and Y. Z. Liu, Continuous preparation of Fe_3O_4 nanoparticles through impinging stream-rotating packed bed reactor and their electrochemistry detection toward heavy metal ions, *J. Alloys Compd.*, 2016, **671**, 354–359.

32 X. J. Han, S. F. Zhou, H. L. Fan, Q. X. Zhang and Y. Q. Liu, Effect of morphology of α-MnO_2 nanocrystals on electrochemical detection of toxic metal ions, *J. Electroanal. Chem.*, 2015, **755**, 203–209.

33 Q. X. Zhang, D. Pneg and X. J. Huang, Mesoporous $MnFe_2O_4$ nanocrystal clusters for electrochemistry detection of lead by stripping voltammetry, *J. Electroanal. Chem.*, 2015, **684**, 1–7.

34 M. Lin, M. Cho, W.-S. Choe and Y. Lee, Electrochemical detection of lead ion based on a peptide modified electrode, *Electroanalysis*, 2016, **28**, 998–1002.

35 A. Chira, B. Bucur, M. P. Bucur and G. L. Radu, Electrode modified with nanoparticles composed of 4,4′-bipyridine-silver coordination polymer for sensitive determination of Hg(II), Cu(II) and Pb(II), *New J. Chem.*, 2014, **38**, 5641–5646.

36 Y. Wei, R. Yang, X. Y. Yu, L. Wang, J. H. Liu and X. J. Huang, Stripping voltammetry study of ultra-trace toxic metal ions on highly selectively adsorptive porous magnesium oxide nanoflowers, *Analyst*, 2012, **137**, 2183–2191.

37 M. K. Bojdi, M. H. Mashhadizadeh, M. Behbahani, A. Farahani, S. S. H. Davarani and A. Bagheri, Synthesis, characterization and application of novel lead imprinted polymer nanoparticles as a high selective electrochemical sensor for ultratrace determination of lead ions in complex matrixes, *Electrochim. Acta*, 2014, **136**, 59–65.

